

Published in final edited form as:

*Integr Biol (Camb)*. 2013 January ; 5(1): . doi:10.1039/c2ib20125a.

## Immune Stimulating Photoactive Hybrid Nanoparticles for Metastatic Breast Cancer†

Sean Marrache<sup>a,1</sup>, Joshua H. Choi<sup>a,1</sup>, Smanla Tundup<sup>c</sup>, Dillon Zaver<sup>a</sup>, Donald A. Harn<sup>c</sup>, and Shanta Dhar<sup>a,b</sup>

<sup>a</sup>Nano Therapeutics Research Lab, Department of Chemistry, University of Georgia, Athens, GA 30602, USA

<sup>b</sup>Department of Physiology and Pharmacology, College of Veterinary Medicine, University of Georgia, Athens, GA 30602, USA

<sup>c</sup>Department of Infectious Diseases, College of Veterinary Medicine, University of Georgia, Athens, GA 30602, USA

### Abstract

A therapeutic technology that combines the phototoxic and immune-stimulating ability of photodynamic therapy (PDT) with the widespread effectiveness of the immune system can be very promising to treat metastatic breast cancer. We speculated that the knowledge of molecular mechanisms of existing multi-component therapies could provide clues to aid the discovery of new combinations of an immunostimulant with a photosensitizer (PS) using a nanoparticle (NP) delivery platform. Therapeutic challenges when administering therapeutic combinations include the choice of dosages to reduce side effects, the definitive delivery of the correct drug ratio, and exposure to the targets of interest. These factors are very difficult to achieve when drugs are individually administered. By combining controlled release polymer-based NP drug delivery approaches, we were able to differentially deliver zinc phthalocyanine (ZnPc) based PS to metastatic breast cancer cells along with CpG-ODN, a single-stranded DNA that is a known immunostimulant to manage the distant tumors in a temporally regulated manner resulting in more effective management of deadly metastatic breast cancer. We encapsulated ZnPc which is a long-wavelength absorbing PS within a polymeric NP core made up of poly(D,L-lactic-co-glycolic acid)-*b*-poly(ethylene glycol) (PLGA-*b*-PEG). After coating the outside of the polymeric core with gold NPs (AuNPs), we further modified the AuNP surface with CpG-ODN. In vitro cytotoxicity using 4T1 metastatic mouse breast carcinoma cells shows significant photocytotoxicity of the hybrid NPs containing both ZnPc and CpG-ODN after irradiation with a 660 nm LASER light and this activity was remarkably better than either treatment alone. Treatment of mouse bone marrow derived dendritic cells with the PDT-killed 4T1 cell lysate shows that the combination of PDT with a synergistic immunostimulant in a single NP system results in significant immune response, which can be used for the treatment of metastatic cancer.

### Introduction

The management of metastatic breast cancer remains a therapeutic challenge.<sup>1</sup> An ideal cancer treatment should not only cause tumor regression and eradication but also induce a

†Electronic supplementary information (ESI) available.

© The Royal Society of Chemistry [year]

shanta@uga.edu; Fax: +1 706 542-9454; Tel: +1 706 542-1012.

<sup>1</sup>S.M. and J. H. C. contributed equally to this work.

systemic antitumor immunity for control of metastatic tumors and long-term tumor resistance. This can be achieved by using the immune system as a weapon to recognize the tumor antigen so that once the primary tumor is eliminated, metastases will also be destroyed. Earlier success in applying the immune system to metastatic cancer, as well as the limited contributions from conventional chemo or radiation therapy makes metastatic cancer a focus for contemporary development of novel treatment options.<sup>2</sup> The main pillars of cancer treatment chemotherapy, surgery, and radiation therapy are known to suppress the immune system.<sup>3</sup> The only cancer treatment that stimulates anti-tumor immunity is photodynamic therapy (PDT).<sup>3-4</sup> PDT involves administration of a photosensitizer (PS) followed by illumination of the tumor with a long wavelength (600-800 nm) light producing reactive oxygen species (ROS) resulting in vascular shutdown, cancer cell apoptosis, and the induction of a host immune response.<sup>5</sup> The exact mechanism involved in the PDT-mediated induction of anti-tumor immunity is not yet understood. Possible mechanisms include alterations in the tumor microenvironment by stimulating pro-inflammatory cytokines and direct effects of PDT on the tumor that increases immunogenicity.<sup>3</sup> PDT can increase dendritic cells (DC) maturation and differentiation, which leads to the generation of tumor specific cytotoxic CD8 T cells, that can destroy distant deposits of untreated tumor (Fig. 1).<sup>3, 6</sup>

There are increasing number of studies showing that immunoadjuvants when injected intratumorally can produce a similar infiltration of leukocytes into the tumor.<sup>3</sup> Immunoadjuvants are frequently prepared from microbial cells and are thought to act via Toll-like receptors (TLRs)<sup>7</sup> present on macrophages and DCs. This indicates that a combination of PDT with a DC activating agent that can act as an agonist of TLR might be promising for the treatment of metastatic tumor. There are few reports of combinations of PDT with microbial derived products potentiating tumor response and leading to long-term anti-tumor immunity.<sup>3, 8</sup> However, thus far administrating the immunoadjuvants as separate constructs by intratumoral injection has only been explored to combine PDT with immunotherapy<sup>9</sup>, their use as a single construct should receive careful consideration. Nanotechnology-based differential combination therapy can be emphasized as a promising strategy for metastatic breast cancer. By combining controlled release nanoparticles (NPs), PDT, and immune activation, we aimed to differentially deliver PS with synergistic immunoadjuvants in a temporally regulated manner resulting in a safer and more effective management of the deadly form of metastatic breast cancer. Here we report a highly advanced biodegradable hybrid NP platform for proof-of-concept demonstration for such a technology (Fig. 2). Polymeric NPs of poly (lactide-*co*-glycolide)-*b*-polyethyleneglycol (PLGA-*b*-PEG) block copolymers are especially promising as drug delivery vehicles.<sup>10</sup> The use of PLGA and PEG polymers in the Food and Drug Administration (FDA) approved products makes these biomaterials ideal for the development of new therapeutics. We used zinc(II) phthalocyanine (ZnPc)<sup>11</sup> as a PS because of its high optical absorption coefficient in the 600 to 800 nm phototherapeutic window, which is higher than the FDA approved PDT drug photofrin®.<sup>2</sup> We encapsulated the PS inside PLGA-*b*-PEG polymeric NPs and modified the surface of the polymeric core with gold NPs (AuNPs) by using non-covalent interactions. For immune stimulation, the surface of the AuNPs was utilized to introduce 5'-purine-purine/T-CpG-pyrimidine-pyrimidine-3'-oligodeoxynucleotides (CpG-ODN) as a potent DC activating agent.<sup>12</sup>

## Materials and methods

All chemicals were used without further purification unless otherwise noted. PLGA-COOH of inherent viscosity of 0.18 dL/g was purchased from Lactel. NH<sub>2</sub>-PEG-NH<sub>2</sub> (MW 2000) was obtained from JenKem USA. 4-dimethylaminopyridine (DMAP), N,N'-dicyclohexylcarbodiimide (DCC), and 3-(4,5-dimethylthiazol-2-yl)-2,5-diphenyltetrazolium

bromide (MTT) were purchased from Sigma-Aldrich. AuNPs of size 5 nm ( $5 \times 10^{13}$  particles/mL) were purchased from BBInternational. Phosphorothioate oligonucleotide CpG-ODN-1826 of sequence 5'-TCCATGACGTTCTGACGTT-3' was purchased from Midland certified reagent company (Midland, Tex.). Granulocyte-macrophage colony-stimulating factor (GM-CSF) was purchased from R&D systems. Cytokines were tested using BD OptEIA mouse enzyme-linked immunosorbent assay (ELISA) kits. Distilled water was purified by passage through a Millipore Milli-Q Biocel water purification system (18.2 M $\Omega$ ) containing a 0.22  $\mu$ m filter. Dynamic light scattering (DLS) measurements for size, zeta potential, and polydispersity index (PDI) were carried out using a Malvern Zetasizer Nano ZS system.  $^1\text{H}$  and  $^{13}\text{C}$  NMR spectra were recorded on a 400 MHz Varian NMR spectrometer. Gel permeation chromatographic (GPC) analyses were performed on Shimadzu LC20-AD prominence liquid chromatographer equipped with a RI detector, molecular weights were calculated using a conventional calibration curve constructed from narrow polystyrene standards. Optical measurements were carried out on a NanoDrop 2000 spectrophotometer. HPLC analyses were made on an Agilent 1200 series instrument equipped with a multi-wavelength UV-visible detector. Transmission electron microscopy (TEM) images were taken in a FEI Tecnai 20 TEM microscope. LASER irradiation was performed using a Melles Griot 660 nm 56 ICS series diode laser equipped with a fiber optic cable in a dark environment.

### Cell Line and Cell Culture

The BALB/c mammary adenocarcinoma 410.4 sub-line 4T1 cells from the American Type Culture Collection (ATCC) were grown in RPMI 1640 media containing HEPES, glutamine, sodium pyruvate, 10% fetal bovine serum (FBS), 100 U/mL penicillin, and 100  $\mu$ g/mL streptomycin at 37 °C in 5% CO<sub>2</sub>. Cells were passed every 3 days and restarted from the frozen stocks upon reaching pass number 20.

### Animals

Animals were obtained from Jackson Laboratory and handled in accordance with “The guide for the Care and Use of Laboratory Animals” of American Association for Accreditation of Laboratory Animal Care (AALAC), Animal Welfare Act (AWA), and other applicable federal and state guidelines. All animal work presented here was approved by Institutional Animal Care and Use Committee (IACUC) of University of Georgia.

### Synthesis of PLGA-*b*-PEG-NH<sub>2</sub>

PLGA-*b*-PEG-NH<sub>2</sub> was synthesized by using an amide coupling reaction. NH<sub>2</sub>-PEG-NH<sub>2</sub> (0.7 g, 0.35 mmol), PLGA-COOH (0.8 g, 0.12 mmol), and DMAP (0.16 g, 1.32 mmol) in 10 mL dry CH<sub>2</sub>Cl<sub>2</sub> was set to stir on ice. DCC (34.1 mg, 0.17 mmol) in 1 mL dry CH<sub>2</sub>Cl<sub>2</sub> was added drop wise to the solution. The solution was warmed to room temperature and stirred over night. It was then filtered to remove the dicyclohexylurea byproduct, precipitated using a mixture of 50:50 methanol-diethyl ether, isolated via centrifugation (5000 rpm, 4 °C, 10 min), and lyophilized overnight. PLGA-*b*-PEG-NH<sub>2</sub> was isolated as a white solid in 29% yield.  $^1\text{H}$  NMR (CHCl<sub>3</sub>-*d*):  $\delta$  5.3 [m, (OCHCH<sub>3</sub>C(O))], 4.9 [m, (OCH<sub>2</sub>C(O))], 3.6 [s, (OCH<sub>2</sub>CH<sub>2</sub>)], 1.9 [m, (CH<sub>3</sub>CH)].  $^{13}\text{C}$  NMR (CHCl<sub>3</sub>-*d*):  $\delta$  169.6, 166.5, 66.0, 61.1, 60.9, 16.9, 15.5. GPC: M<sub>n</sub> = 7,070 g/mol, M<sub>w</sub> = 8,540 g/mol, PDI = 1.21.

### Synthesis of ZnPc-Poly-NPs

ZnPc-encapsulated NPs (ZnPc-Poly-NPs) were prepared by using the nanoprecipitation method.<sup>10b</sup> PLGA-*b*-PEG-NH<sub>2</sub> (50 mg/mL) and ZnPc, at varying percent weight with respect to the polymer weight, were dissolved in DMF. This mixture was slowly added to water over a period of 10 min. The NPs formed were stirred at room temperature for 2-3 h

and washed 3 times with nanopure water using Amicon ultracentrifugation filtration membranes with a molecular weight cutoff of 100 kDa (3000 rpm, 4 °C). The NP size, PDI, and zeta potential were obtained by DLS measurements. Size and the morphology of the NPs were further confirmed by TEM. The ZnPc content in the NPs was measured by HPLC.

### Synthesis of Au-ZnPc-Poly-NPs

An aqueous suspension of 1 mL ZnPc-Poly-NPs was added to a 2 mL aqueous solution of citrate coated AuNPs of size 5 nm and allowed to sit for 4 h at room temperature. The NPs were characterized by DLS, TEM, and UV-Vis spectroscopy.

### Synthesis of CpG-ODN-Au-ZnPc-Poly-NPs

CpG-ODN of sequence 5'-TCCATGACGTTTCCTGACGTT-3' with a disulfide bond in the 5' end was deprotected according to the manufacturer's protocol. Briefly, to a solution of CpG-ODN in 0.1 M triethylammonium acetate buffer (pH 6.5), an aqueous solution of 0.1 M DTT was added and incubated at room temperature for 30 min. The deprotected CpG-ODN was purified using a 50 mg C18 Sep-Pak cartridge (Waters, Milford, MA) equilibrated in and eluted with DNase/RNase-free distilled water. The concentration of the CpG-ODN was measured by UV-Vis spectroscopy. Au-ZnPc-Poly-NPs were added to an equivalent volume of 10% (v/v) Tween 20 at room temperature. Then CpG-ODN was added (210  $\mu$ L, 105  $\mu$ g/mL) and incubated at room temperature in a shaker for 20 h. CpG-ODN-Au-ZnPc-Poly-NPs were washed 3 times using Amicon ultracentrifugation filtration membranes with a molecular weight cutoff of 100 kDa (3000 rpm, 4 °C). Finally, NPs were resuspended in water and analyzed by DLS. NP solutions were analyzed by UV-Vis after dissolving the polymeric core using 1 M NaOH for determination of encapsulated ZnPc content or dissolving the gold core with 0.6 M KI for quantification of conjugated CpG-ODN.

### Determination of ZnPc loading and encapsulation efficiency

ZnPc loading and encapsulation efficiency (EE) were calculated by dissolving the polymer core by mixing equal portions of the NP solution and 1 N NaOH, followed by dilution with a 50:50 water:acetonitrile mixture, and subsequent HPLC analysis (wavelength: 670 nm). ZnPc loading is defined as the mass fraction of PS in the NPs, whereas EE is the fraction of initial PS used for encapsulation by the NPs during nanoprecipitation.<sup>13</sup>

### MTT Assay

The phototoxic behavior of all the NPs was evaluated using the MTT assay against 4T1 cells. 4T1 cells (1500 cells/well) were seeded on a 96-well plate in 100  $\mu$ L of RPMI medium and incubated for 24 h. The cells were treated with NPs at varying concentrations (with respect to ZnPc) and incubated for 2 h at 37 °C. The cells were then irradiated with a 660 nm LASER (power 20 mW) with a fiber optics for 5 min per well. Irradiated cells were incubated for 12 h at 37 °C, medium was changed after 12 h, and the cells were incubated for additional 60 h. The cells were then treated with 20  $\mu$ L of MTT (5 mg/mL in PBS) for 5 h. The medium was removed, the cells were lysed with 100  $\mu$ L of DMSO, and the absorbance of the purple formazan was recorded at 550 nm using a Bio-Tek Synergy HT microplate reader. Each well was performed in triplicate. All experiments were repeated three times. Cytotoxicity was expressed as mean percentage increase relative to the unexposed control  $\pm$  SD. Control values were set at 0% cytotoxicity or 100% cell viability. Cytotoxicity data (where appropriate) was fitted to a sigmoidal curve and a three parameters logistic model was used to calculate the  $IC_{50}$ , which is the concentration of the agent causing 50% inhibition in comparison to untreated controls. The mean  $IC_{50}$  is the concentration of agent that reduces cell growth by 50% under the experimental conditions and is the average from at least three independent measurements that were reproducible and

statistically significant. The IC<sub>50</sub> values are reported at ±95% confidence intervals (±95% CI). This analysis was performed with Graph Pad Prism (San Diego, U.S.A) software.

### Generation of bone marrow derived dendritic cells

Bone marrow derived dendritic cells (BMDCs) were isolated from 6-8 weeks old C57BL/6 mice. Mice were euthanized and bone marrows were isolated by flushing mouse femurs in RPMI. The harvested cells were centrifuged at 1250 rpm for 10 min and the resulting pellet was resuspended in ice-cold buffer (2 mL) to lyse erythrocytes. The cells were counted, resuspended, and transferred to petri dishes at the final concentration of  $1.5 \times 10^6$  cells/mL. To this culture GM-CSF at 20 ng/mL was added to generate BMDCs. Media was changed on days 2, 4 and 6 and cells were used on day 7.

### Preparation of PDT treated 4T1 cells

4T1 cells were plated at the concentration of  $4 \times 10^5$  cells/well in six well plates and allowed to grow for 24 h. On the next day, the cells were incubated with 10 nM ZnPc, 6.16 nM CpG-ODN, a mixture of 10 nM ZnPc and 6.16 nM CpG-ODN, 10 nM ZnPc-Poly-NPs, 10 nM Au-ZnPc-Poly-NPs, 10 nM CpG-ODN-Au-ZnPc-Poly-NPs for 2 h, and irradiated with a 660 nm LASER light for 5 min. Cells were left in the culture for 12 h at 37 °C and PDT lysates were used for stimulation of the BMDCs.

### Stimulation of BMDCs with supernatants from PDT treated tumor cells

The PDT-lysates obtained 24 h post PDT treatment of 4T1 cells were added to freshly prepared BMDCs. Additionally lipopolysaccharide (LPS) alone (100 ng/mL) or CpG-ODN alone (1 µg/mL or 10 µg/mL) was added to the DC cultures as controls. DCs were incubated with the supernatants for 12 h at 37 °C and the supernatants were harvested for further studies.

### Immune response by ELISA

ELISA was performed using the supernatants harvested from BMDC culture to measure the levels of cytokines IL-2, IL-4, IL-6, IL-10, IL-12, TNF- $\alpha$ , and IFN- $\gamma$  according to manufactures protocol. Briefly, the cell supernatants were incubated with antibody-coated plates for 2 h at room temperature. This was immediately followed by washings and sequential incubations with the biotin-conjugated detection antibody and streptavidinhorseradish peroxidase (HRP) solution. Finally, the ELISA was developed by adding the substrate (100 µL/well) to each well followed by a stop solution. The absorbance was recorded at 450 nm using a BioTek Synergy HT well plate reader.

## Results

### Synthesis of the polymer and construction of the NPs

To co-deliver PS and an immunoadjuvant using a single NP construct and to obtain adequate control over encapsulation of the hydrophobic PS, ZnPc, we synthesized a biodegradable polymer with a terminal -NH<sub>2</sub> group (PLGA-*b*-PEG-NH<sub>2</sub>) via an amide coupling of PLGA-COOH with NH<sub>2</sub>-PEG-NH<sub>2</sub> using DCC/DMAP as coupling agents. This polymer was characterized by <sup>1</sup>H and <sup>13</sup>C NMR spectroscopy (Figs. S1 and S2, ESI<sup>†</sup>). Purity, molecular weights, and PDI of the polymer were determined by GPC measurements using tetrahydrofuran mobile phase (Table S1, ESI<sup>†</sup>). These results are consistent with previously reported data for PLGA-*b*-PEG-COOH polymer.<sup>14</sup>

<sup>†</sup>Electronic supplementary information (ESI) available.



Synthesis of the NPs with PLGA-*b*-PEG-NH<sub>2</sub> was achieved by the nanoprecipitation method.<sup>10a, b</sup> PLGA-*b*-PEG-NH<sub>2</sub> was dissolved in a water miscible solvent DMF and then added drop wise into an aqueous solution, generating NPs. The properties of the encapsulated NPs were characterized by DLS to give the hydrodynamic diameter, zeta potential, and PDI of each preparation. To optimize the size and loading, a series of encapsulated NPs were prepared by varying the weight percentage of ZnPc to polymer (%w/w) and by using PEG of various molecular masses. When the DMF solution of the polymer and ZnPc was added to water, the mixture became turbid, indicating the formation of NPs. However, depending on the conditions, the final suspension contained a larger or smaller amount of larger polymeric aggregates either dispersed in the aqueous phase or adhering to the flask wall or to the magnetic stirring bar. In this way, we found that PLGA of inherent viscosity 0.18 dL/g in hexafluoroisopropanol affords the most suitable encapsulated NPs. It is worth noting that measurements of NP size made on three different batches produced under identical conditions fell within a range of 10% variation, indicating a good reproducibility. The loading efficiencies of ZnPc at various added weight percentage with respect to the polymer weight are given in Fig. 3. The size of the NPs increased with ZnPc loading (Fig. 3). For all in vitro studies, we used encapsulated NPs containing 30% ZnPc added with respect to the polymer.

For the synthesis of the hybrid NPs, anionic ligand citrate stabilized AuNPs were used. This allowed an effective binding between the positively charged NH<sub>2</sub> groups of the polymeric ZnPc-Poly-NPs and the negatively charged citrate groups of the AuNPs. The formation of these hybrid Au-ZnPc-Poly-NPs was evident from the DLS measurement, which shows a change in the zeta potential of the polymeric NPs from positive to a negative value (Fig. 3). The addition of ZnPc-Poly-NPs to AuNPs did not cause any aggregation (Fig. 3).

We modified the AuNP surface with CpG-ODN with a 5'-modified -SH group.<sup>15</sup> We were able to load high concentration of CpG-ODN on the AuNP surface as evident from the UV-Vis study. CpG-ODN adsorption stabilizes the hybrid NPs and the steric repulsion of the NPs prevents flocculation as evident from the decrease in size and PDI (Fig. 3). Negative zeta potential of Au-ZnPc-Poly-NPs decreased with the formation of CpG-ODN-Au-ZnPc-Poly-NPs.

### In vitro stability of the hybrid NPs

In vitro stability of NPs can be defined relative to changes in hydrodynamic size and surface charge in response to changes in the sample environment. The key physicochemical properties, nanoparticle size, surface zeta potential, and morphology determine the in vivo stability profiles. We checked the short-term stability of an aqueous suspension of CpG-ODN-Au-ZnPc-Poly-NPs by storing at 4 °C for 30 days and evaluating the size distribution and zeta potential (Table S2, ESI<sup>†</sup>). The diameter of the hybrid NPs decreases day after day. The mean size decreased from 186 nm to ~90 nm after 30 days and the surface charge changes from ~ -10 mV to -20 mV (Table S2, ESI<sup>†</sup>).

### In vitro phototoxicity on metastatic breast cancer cells

The photodynamic activities of ZnPc-Poly-NPs, Au-ZnPc-Poly-NPs, and CpG-ODN-Au-ZnPc-Poly-NPs were investigated against 4T1 cell line using a 660 nm laser. In parallel, cells were incubated with all the constructs without illumination to serve as dark controls (Fig. 4). None of these constructs show any phototoxicity in the dark. The induction of cell death was both light and ZnPc-dose dependent. Two hours following the incubations, cells were illuminated with a 660 nm LASER light for 5 min per well. The mortality of post-PDT cultures was determined following the MTT assay. A higher phototoxic effect was observed with CpG-ODN-Au-ZnPc-Poly-NPs (IC<sub>50</sub>; 2.8 nM) than the ZnPc-Poly-NPs (IC<sub>50</sub>; 15 nM),

Au-ZnPc-Poly-NPs ( $IC_{50}$ ; 6 nM) or free ZnPc ( $IC_{50}$ ; 317 nM) (Fig. 4). Control cells incubated with unconjugated AuNPs did not display any significant cell death after illumination. Thus, under these *in vitro* conditions we can exclude the possibility that any case of cell death is due to the photothermal activity of the AuNPs. Interestingly, the efficacy of free ZnPc was lower than that for hybrid NPs containing ZnPc in the polymeric core and CpG-ODN immobilized on the AuNP surface. This enhancement in photodynamic efficacy is likely to be a consequence of synergistic effect between ZnPc and CpG-ODN when delivered in a single construct.

### In vitro antitumor immunity after PDT

We incubated bone marrow derived immature DCs isolated from C57BL/6 mice with CpG-ODN or with LPS, a TLR4 agonist generally employed as a positive factor to stimulate and activate DCs, as positive controls and with PDT killed 4T1 cell lysates. We used ELISA analysis to assess the immune response by measuring the levels of several proinflammatory cytokines (Fig. 5). When CpG-ODN-Au-ZnPc-Poly-NP treated PDT killed 4T1 tumor cell lysate was incubated with DCs, there was a synergistic increase in the production of IL-2, IL-6, IL-12, and TNF- $\alpha$  and these levels were either comparable or above the level of activation achieved with LPS (Fig. 5). However when a combination of free CpG-ODN and ZnPc, or ZnPc-Poly-NP treated PDT killed 4T1 cell lysates were incubated with DCs, all the cytokine levels were below than the levels observed for CpG-ODN-Au-ZnPc-Poly-NPs. CpG-ODN alone had only a slight effect in secretion of these cytokines. These data suggest that a combination of CpG-ODN and a photosensitizer in a single NP construct can prime DC to recognize and phagocytose PDT killed tumor cells, and that this phagocytosis can lead to DC maturation and activation. Our construct causes activation of a specific and systemic immune response after PDT, which may result in not only further destruction of remaining local tumor cells but also the prevention of possible recurrence. The antitumor efficacy of PDT was further enhanced through an effective immunoadjuvant CpG-ODN to expand its usefulness for a possible control of distant metastasis. The concentrations of other cytokines, IL-4, IL-10, and IFN- $\gamma$  were not changed compared with those of dark controls. Control experiments with various NPs without encapsulated ZnPc showed no significant activation after PDT or in the dark except for empty-CpG-ODN-Au-Poly-NPs, which showed immune response comparable to free CpG-ODN (Fig. S3, ESI<sup>†</sup>).

### Discussion

We designed a hybrid NP to load both PS and an immunoadjuvant. A hydrophobic photosensitizer is required to achieve high loading inside polymeric NPs. ZnPc, which is hydrophobic provided us with the required solubility needed for encapsulation inside the hydrophobic core of biodegradable PLGA-*b*-PEG-NH<sub>2</sub> NPs. The terminal NH<sub>2</sub> groups were used as convenient handles for coupling of anionic citrate stabilized AuNPs through non-covalent electrostatic interaction. The formation of the AuNP coated NPs were evident from the changes in the zeta potential and appearance of the surface plasmon band at 520 nm in the absorption spectrum. Addition of ZnPc-Poly-NPs to AuNPs did not cause any visible aggregation (Fig. 3A). This was followed photometrically by observing the decrease and/or red shift of the plasmon absorption band of AuNPs at ~520 nm. Absence of any change in the 520 nm band confirms that this hybrid NP system is stable (Fig. 3C). Formation of the hybrid NPs were also evident from the TEM images (Fig. 3B). We adopted this non-covalent attachment approach with the goal that ZnPc inside the polymeric core will be released inside the cancer cells, whereas CpG-ODN containing AuNPs will be detached from the polymeric NPs and can be engaged in activating tumor associated DCs after PDT. AuNP surface has many advantageous properties such as chemical stability, a highly electron dense core, and ease of conjugation to oligonucleotides.<sup>15</sup> CpG-ODNs are powerful

stimulators of innate as well as adaptive immune responses; however, the immunopotency of CpG-ODN is less when given in the free form.<sup>16</sup> Our technology of mobilizing CpG-ODN on the AuNP surface for immediate release after PDT specifically targets CpG-ODN for uptake by the immune cells. Immobilization of CpG-ODN was confirmed by UV-vis spectroscopy (Fig. 3C). In CpG-ODN-Au-ZnPc-Poly-NPs, the Au core masks DNA absorption band. The DNA band appears at 260 nm upon dissolution of the Au core by KI and confirms the presence of CpG-ODN in the hybrid NPs (Fig. 3C). We have used a nuclease-resistant phosphorothioate backbone, which is known to improve the stability of an optimal CpG-ODN and its ability to activate B cells and DCs, and to induce cytokine production.<sup>17</sup> However, it is important to note that the phosphorothioate backbone also reduces the ability to activate natural killer (NK) cells and thus may be less useful for tumor immunotherapy applications that depend on these effector cells.<sup>18</sup>

NP stability in aqueous solution is critical for their utility as a drug delivery vehicle in vivo. NP size is one of the most critical parameters that determine systemic circulation lifetime and NP ability to passively accumulate in tumor tissues and NPs with a size range of 10-150 nm are on demand for systemic drug delivery.<sup>19</sup> Surface zeta potential is also a critical factor to determine both in vitro and in vivo stability of the NPs. An aqueous suspension of 5 mg/mL CpG-ODN-Au-ZnPc-Poly-NPs stored at 4 °C for 1 month did not show observable aggregation (Table S2, ESI<sup>†</sup>). Such excellent stability of these NPs renders them suitable for biomedical applications in vivo. However, when NP concentration is too high, there is always a chance of aggregation. Total volume fraction of NPs in the solution, PLGA length, PEG ratio, and PEG surface density can be varied to tune NP stability for possible in vivo applications.

We have used a mouse mammary tumor cell line 4T1, one of only a few breast cancer models with the capacity to metastasize, to test the in vitro photodynamic activity and PDT mediated anti tumor immunity with our construct.<sup>20</sup> It is poorly immunogenic, spontaneously metastatic, and highly malignant. We carried out a series of in vitro cytotoxicity assays to evaluate the potential of our engineered hybrid NP construct containing both ZnPc and CpG-ODN in metastatic breast cancer using 4T1 cells and directly comparing its efficacy to that of free ZnPc, AuNPs, ZnPc-Poly-NPs, and Au-ZnPc-Poly-NPs. As represented in Fig. 4, CpG-ODN-Au-ZnPc-Poly-NPs are highly phototoxic to 4T1 cells, having an IC<sub>50</sub> value of 2.8 nM when irradiated with a 660 nm LASER for only 5 min. This construct has no toxicity in the dark. Under similar conditions, NPs containing the photosensitizer alone (ZnPc-Poly-NPs) have an IC<sub>50</sub> value of 15 nM, and for free ZnPc the value with these cells is 317 nM, ~2 orders of magnitude less effective. Significant phototoxicity of our construct is indicative of the potential of a synergistic combination of a photosensitizer and an immunoadjuvant in a single delivery platform to treat metastatic breast cancer.

CpG-ODN stimulates B cells, NK cells, DCs, and macrophages, regardless of whether the DNA is in the form of genomic bacterial DNA or in the form of synthetic ODN. The production of high-affinity antibodies and the generation of cytotoxic T cells that provide long-lasting protection characterize the resultant antigen-specific immunity during PDT. The use of CpG-ODN in combination with ZnPc in a single NP construct had a significant immune response after PDT. TLR9 recognizes d(CpG) dinucleotides present in the synthetic CpG-ODN used in our construct. CpG-ODN has strong immunostimulatory activity on murine and human immune cells in vitro and in vivo, such as: induction of tumor specific Th17 response, triggering B cell proliferation, NK cell secretion of IFN- $\gamma$ , increased lytic activity, and macrophage secretion of IFN- $\alpha/\beta$ , IL-6, IL-12, granulocytemonocyte colony-stimulating factor, chemokines, and TNF- $\alpha$ . One important question to answer in designing any combinatory therapy is the order of administration of the respective component



treatments, their local concentration, and the stoichiometric ratio. These parameters are very difficult to control when the components are administered separately. By designing a hybrid NP system, we aimed to provide PDT first followed by release of CpG-ODN for further enhancement of PDT-mediated antitumor immunity. We assumed that the chief role of CpG-ODN is to potentiate phagocytosis of necrotic or apoptotic tumor cells by already present DCs and to induce DC maturation and migration to draining lymph nodes. CpG-ODN activation after PDT will be superior since the PDT induced damage will further enhance over all DC activity when stimulated with CpG-ODN conjugate. The results showed that our combination of ZnPc and CpG-ODN in a single NP construct was significantly better than either treatment alone. Treatment of DCs with PDT-cell lysates and CpG-ODN from a controlled release NP could produce better systemic immune responses due to the creation of potential tumor antigenic fragments before the immune stimulation, which facilitates uptake of antigen presenting cells. The immunosuppressive tumor environment is one of the key players of compromised anti-tumor immune responses. The dominant immunosuppressive cytokines in the tumor microenvironment are IL-10, transforming growth factor, and vascular endothelial growth factor, which inhibit DC maturation/activation.<sup>21</sup> One of the most remarkable finding of our current study is the ability of the hybrid NP formulation to shift the balance at the tumor microenvironment towards immune stimulation, as evidenced by the increase in the level of proinflammatory/Th1-biased cytokines IL-2, IL-6, IL-12, TNF- $\alpha$  and minimal effect in the level of the immunosuppressant such as IL-10 (Fig. 5). A hybrid NP-based delivery of PDT and CpG-ODN can produce effective synergistic response by activating innate and adaptive antitumor immunity, which can be used as a more effective adjuvant for tumor vaccines as well as immunotherapeutic adjuvant.

## Conclusion

We synthesized a hybrid NP system that can be loaded with a photosensitizer and an immunoadjuvant for combination therapy. PLGA-*b*-PEG copolymer functionalized with a terminal -NH<sub>2</sub> group was used to provide a hydrophobic core for effective loading of a photosensitizer, ZnPc. The amine groups from the polymeric NPs, acting as anchors, were utilized to decorate the NP surface with anionic AuNPs and CpG-ODN-based immunoadjuvant was immobilized on the gold surface. Using 4T1 cells as a model for metastatic breast cancer, we demonstrated that the phototoxicity of this hybrid NP containing CpG-ODN and the photosensitizer, ZnPc, is significantly higher than the free PS, PS alone in a NP, or a combination of the PS and the immunoadjuvant in their free forms. We observed involvement of several cytokines in the PDT-induced immune response after treatment with CpG-ODN-Au-ZnPc-poly-NPs. When a mixture of CpG-ODN and ZnPc was used, no significant immune response was seen under similar conditions. These results indicate that the PDT-induced antitumor immune response and its further enhancement using synergistic immunoadjuvant in a suitably designed NP construct might play an important role in successful control of malignant diseases. These results support that a rational choice of an immunostimulant can be an ideal addition to PDT regimen if both the photosensitizer and the immunoadjuvant can be delivered using a single delivery vehicle. These results will play critical roles in building the knowledge required to design NPs to be used for photoimmunotherapy of metastatic cancers.

## Supplementary Material

Refer to Web version on PubMed Central for supplementary material.

## Acknowledgments

We thank Anna Williams for carrying out some preliminary experiments.

Sources of funding

This work was supported by a start-up grant from the National Institutes of Health (P30 GM 092378) and by the Office of the Vice President for Research, UGA to S.D and a grant from the National Institutes of Health (NIH AI056484) to D.H.

## Non-standard abbreviations and acronyms

<b>BMDC</b>	Bone marrow derived dendritic cell
<b>CpG</b>	Unmethylated CpG dinucleotides
<b>DLS</b>	Dynamic light scattering
<b>IL</b>	Interleukins
<b>NP</b>	Nanoparticle
<b>ODNs</b>	Oligodeoxynucleotides
<b>PDT</b>	Photodynamic therapy
<b>PDI</b>	Polydispersity index
<b>PEG</b>	Polyethylene glycol
<b>PLGA</b>	Poly(lactic- <i>co</i> -glycolic acid)
<b>PS</b>	Photosensitizer
<b>TNF</b>	Tumor necrosis factor
<b>ZnPc</b>	Zinc phthalocyanine

## Notes and references

1. DeSantis C, Siegel R, Bandi P, Jemal A. Breast cancer statistics, 2011. *Ca-Cancer J Clin.* 2011; 61:409–418. [PubMed: 21969133]
2. Turcotte S, Rosenberg SA. Immunotherapy for metastatic solid cancers. *Adv Surg.* 2011; 45:341–360. [PubMed: 21954698]
3. Castano AP, Mroz P, Hamblin MR. Photodynamic therapy and anti-tumour immunity. *Nat Rev Cancer.* 2006; 6:535–545. [PubMed: 16794636]
4. Gollnick SO, Owczarczak B, Maier P. Photodynamic therapy and anti-tumor immunity. *Laser Surg Med.* 2006; 38:509–515.
5. Dougherty TJ, Gomer CJ, Henderson BW, Jori G, Kessel D, Korbek M, Moan J, Peng Q. Photodynamic therapy. *J Natl Cancer Inst.* 1998; 90:889–905. [PubMed: 9637138]
6. a Korbek M. Cancer vaccines generated by photodynamic therapy. *Photoch Photobio Sci.* 2011; 10:664–669. b van Duijnhoven FH, Aalbers RIJM, Rovers JP, Terpstra OT, Kuppen PJK. Immunological aspects of photodynamic therapy of liver tumors in a rat model for colorectal cancer. *Photochem Photobiol.* 2003; 78:235–240. [PubMed: 14556309] c Oseroff A. PDT as a cytotoxic agent and biological response modifier: Implications for cancer prevention and treatment in immunosuppressed and immunocompetent patients. *J Invest Dermatol.* 2006; 126:542–544. [PubMed: 16482195]
7. Werling D, Jungi TW. TOLL-like receptors linking innate and adaptive immune response. *Vet Immunol Immunopathol.* 2003; 91:1–12. [PubMed: 12507844]
8. Gollnick SO, Brackett CM. Enhancement of anti-tumor immunity by photodynamic therapy. *Immunol Res.* 2010; 46:216–226. [PubMed: 19763892]

9. a Qiang YG, Yow CMN, Huang Z. Combination of photodynamic therapy and immunomodulation: Current status and future trends. *Med Res Rev.* 2008; 28:632–644. [PubMed: 18161883] b St Denis TG, Aziz K, Waheed AA, Huang YY, Sharma SK, Mroz P, Hamblin MR. Combination approaches to potentiate immune response after photodynamic therapy for cancer. *Photoch Photobio Sci.* 2011; 10:792–801.
10. a Dhar S, Gu FX, Langer R, Farokhzad OC, Lippard SJ. Targeted delivery of cisplatin to prostate cancer cells by aptamer functionalized Pt(IV) prodrug-PLGA-PEG nanoparticles. *Proc Natl Acad Sci USA.* 2008; 105:17356–17361. [PubMed: 18978032] b Dhar S, Kolishetti N, Lippard SJ, Farokhzad OC. Targeted delivery of a cisplatin prodrug for safer and more effective prostate cancer therapy in vivo. *Proc. Natl. Acad. Sci. USA.* 2011; 108:1850–5. [PubMed: 21233423] c Farokhzad OC, Jon SY, Khadelmhosseini A, Tran TNT, LaVan DA, Langer R. Nanoparticle-aptamer bioconjugates: A new approach for targeting prostate cancer cells. *Cancer Res.* 2004; 64:7668–7672. [PubMed: 15520166] d Kolishetti N, Dhar S, Valencia PM, Lin LQ, Karnik R, Lippard SJ, Langer R, Farokhzad OC. Engineering of self-assembled nanoparticle platform for precisely controlled combination drug therapy. *Proc. Natl. Acad. Sci. USA.* 2010; 107:17939–17944. [PubMed: 20921363] e Soppimath KS, Aminabhavi TM, Kulkarni AR, Rudzinski WE. Biodegradable polymeric nanoparticles as drug delivery devices. *J Controlled Rel.* 2001; 70:1–20. f Langer R. Drug delivery. *Drugs on target. Science.* 2001; 293:58–59. [PubMed: 11441170]
11. Ochsner M. Light scattering of human skin: a comparison between zinc (II)-phthalocyanine and photofrin II. *J Photochem Photobiol B.* 1996; 32:3–9. [PubMed: 8725049]
12. a Yamamoto S, Yamamoto T, Nojima Y, Umemori K, Phalen S, McMurray DN, Kuramoto E, Iho S, Takauji R, Sato Y, Yamada T, Ohara N, Matsumoto S, Goto Y, Matsuo K, Tokunaga T. Discovery of immunostimulatory CpG-DNA and its application to tuberculosis vaccine development. *Jpn J Infect Dis.* 2002; 55:37–44. [PubMed: 12082305] b Weeratna RD, Makinen SR, McCluskie MJ, Davis HL. TLR agonists as vaccine adjuvants: comparison of CpG ODN and Resiquimod (R-848). *Vaccine.* 2005; 23:5263–5270. [PubMed: 16081189]
13. Karnik R, Gu F, Basto P, Cannizzaro C, Dean L, Kyei-Manu W, Langer R, Farokhzad OC. Microfluidic platform for controlled synthesis of polymeric nanoparticles. *Nano Lett.* 2008; 8:2906–2912. [PubMed: 18656990]
14. Gu F, Zhang L, Teply BA, Mann N, Wang A, Radovic-Moreno AF, Langer R, Farokhzad OC. Precise engineering of targeted nanoparticles by using self-assembled biointegrated block copolymers. *Proc Natl Acad Sci USA.* 2008; 105:2586–2591. [PubMed: 18272481]
15. Dhar S, Daniel WL, Giljohann DA, Mirkin CA, Lippard SJ. Polyvalent oligonucleotide gold nanoparticle conjugates as delivery vehicles for platinum(IV) warheads. *J Am Chem Soc.* 2009; 131:14652–14653. [PubMed: 19778015]
16. de Jong S, Chikh G, Sekirov L, Raney S, Semple S, Klimuk S, Yuan N, Hope M, Cullis P, Tam Y. Encapsulation in liposomal nanoparticles enhances the immunostimulatory, adjuvant and anti-tumor activity of subcutaneously administered CpG ODN. *Cancer Immunol Immun.* 2007; 56:1251–1264.
17. a Krieg AM, Yi AK, Matson S, Waldschmidt TJ, Bishop GA, Teasdale R, Koretzky GA, Klinman DM. CpG motifs in bacterial-DNA trigger direct B-cell activation. *Nature.* 1995; 374:546–549. [PubMed: 7700380] b Hartmann G, Weiner GJ, Krieg AM. CpG DNA: A potent signal for growth, activation, and maturation of human dendritic cells. *Proc Natl Acad Sci USA.* 1999; 96:9305–9310. [PubMed: 10430938] c Krieg AM, Matson S, Fisher E. Oligodeoxynucleotide modifications determine the magnitude of B cell stimulation by CpG motifs. *Antisense Nucleic A.* 1996; 6:133–139. d Liang H, Nishioka Y, Reich CF, Pisetsky DS, Lipsky PE. Activation of human B cells by phosphorothioate oligodeoxynucleotides. *J Clin Invest.* 1996; 98:1119–1129. [PubMed: 8787674]
18. Ballas ZK, Rasmussen WL, Krieg AM. Induction of NK activity in murine and human cell sby CpG motifs in oligodeoxynucleotides and bacterial DNA. *J Immunol.* 1996; 157:1840–1845. [PubMed: 8757300]
19. a Alexis F, Pridgen E, Molnar LK, Farokhzad OC. Factors affecting the clearance and biodistribution of polymeric nanoparticles. *Mol Pharmaceut.* 2008; 5:505–515. b Kolishetti, N.; Alexis, F.; Pridgen, EM.; Farokhzad, OC. *Nanoplatform-Based Molecular Imaging.* John Wiley & Sons, Inc.; 2011. p. 75-104.

20. Morecki S, Yacovlev L, Slavin S. Effect of indomethacin on tumorigenicity and immunity induction in a murine model of mammary carcinoma. *Int J Cancer*. 1998; 75:894–899. [PubMed: 9506535]
21. a Mesa C, Fernandez LE. Challenges facing adjuvants for cancer immunotherapy. *Immunol Cell Biol*. 2004; 82:644–650. [PubMed: 15550123] b Morisaki T, Katano M, Ikubo A, Anan K, Nakamura M, Nakamura K, Sato H, Tanaka M, Torisu M. Immunosuppressive cytokines (IL-10, TGF-beta) genes expression in human gastric carcinoma tissues. *J Surg Oncol*. 1996; 63:234–239. [PubMed: 8982367]

### **Insight, innovation, integration**

Benefitting from a unique use among expertise in different areas, chemistry, immunology, and nanotechnology, we have developed an engineered nanoparticle (NP) platform, which uses a combination of photodynamic therapy (PDT) and the immune system for effective management of metastatic breast cancer. Chemotherapy remains the backbone for systemic therapy to treat breast cancer. However, in the setting of metastatic form, single agent based chemotherapy is not effective and it is reasonably apparent that the search for a single-component therapeutic may not be useful. Nanotechnology holds significant promise as the next generation cancer therapeutic modality. The clinical utility of this multi-drug NP could make a major advance for the care of women with metastatic breast cancer.



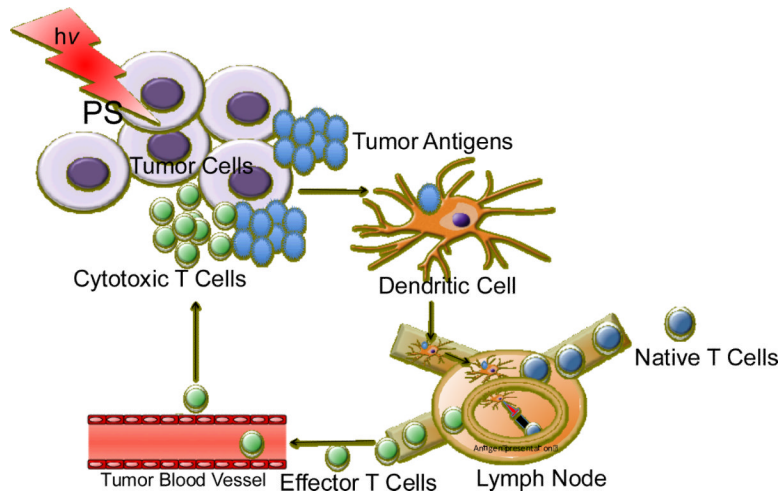


**Fig. 1.**  
Phagocytosis of tumor antigens by DCs after PDT.

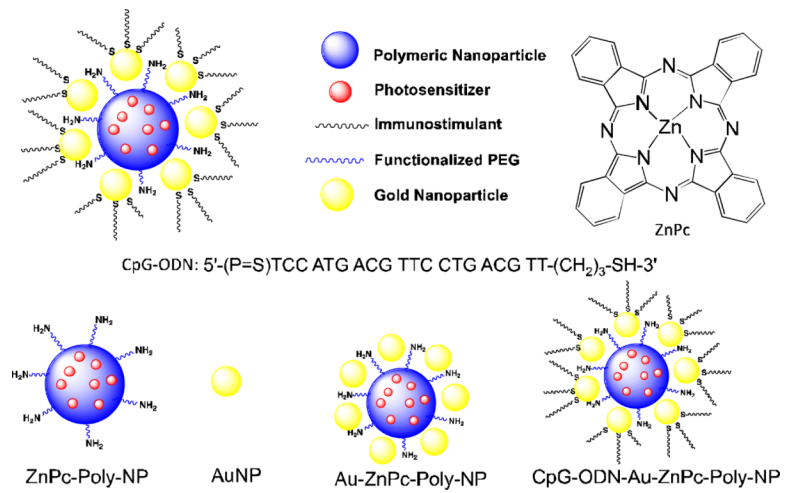


**Fig. 2.** Schematic diagram of the NP platform for combination therapy of metastatic breast cancer.

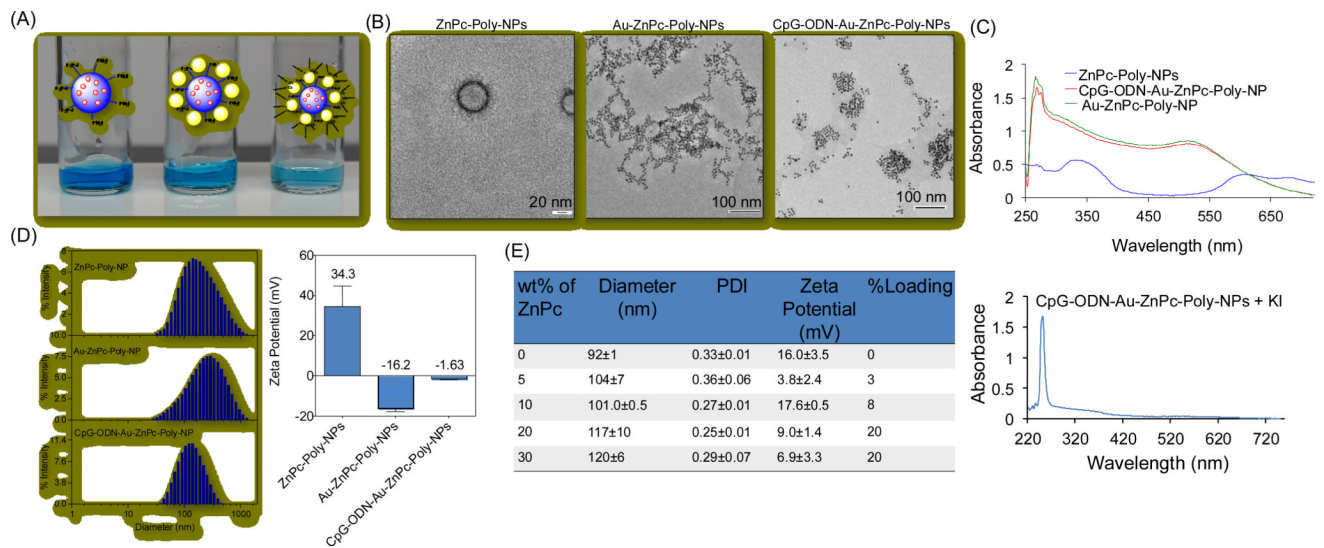


**Fig. 3.** Characterization of hybrid NP constructs. (A) Photographs of NP suspensions showing no visible aggregation. (B) TEM images of ZnPc-Poly-NPs, Au-ZnPc-Poly-NPs, and CpG-ODN-Au-ZnPc-Poly-NPs. (C) Characterization of hybrid NPs by UV-Vis spectroscopy. (D) Hydrodynamic diameter and zeta potential of the NPs by DLS measurements. (E) Sizes, PDI, zeta potential, and loading of ZnPc in the PLGA-*b*-PEG-NH<sub>2</sub> with varied ZnPc percent weight.

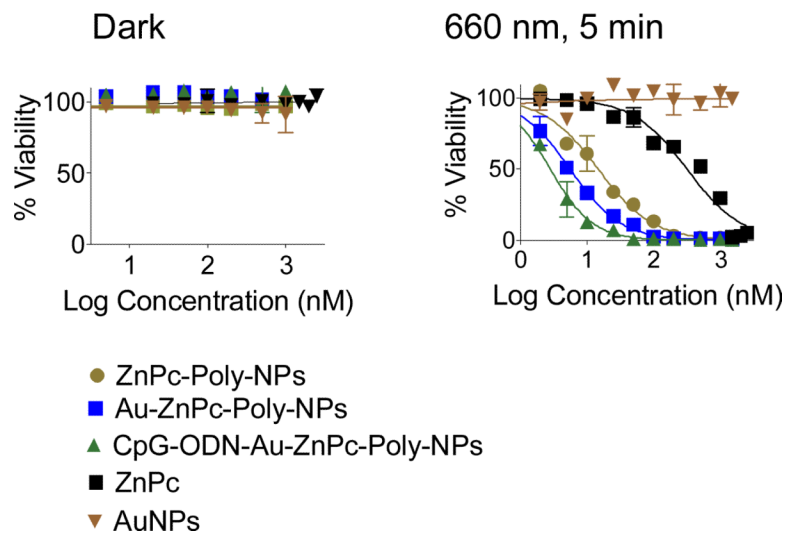


**Fig. 4.** Cytotoxicity profiles of ZnPc-Poly-NPs, Au-ZnPc-Poly-NPs, and CpG-ODN-Au-ZnPc-Poly-NPs in 4T1 cells in the dark (left) and after 5 min exposure with a 660 nm LASER (right). Free ZnPc and AuNPs were used as controls.

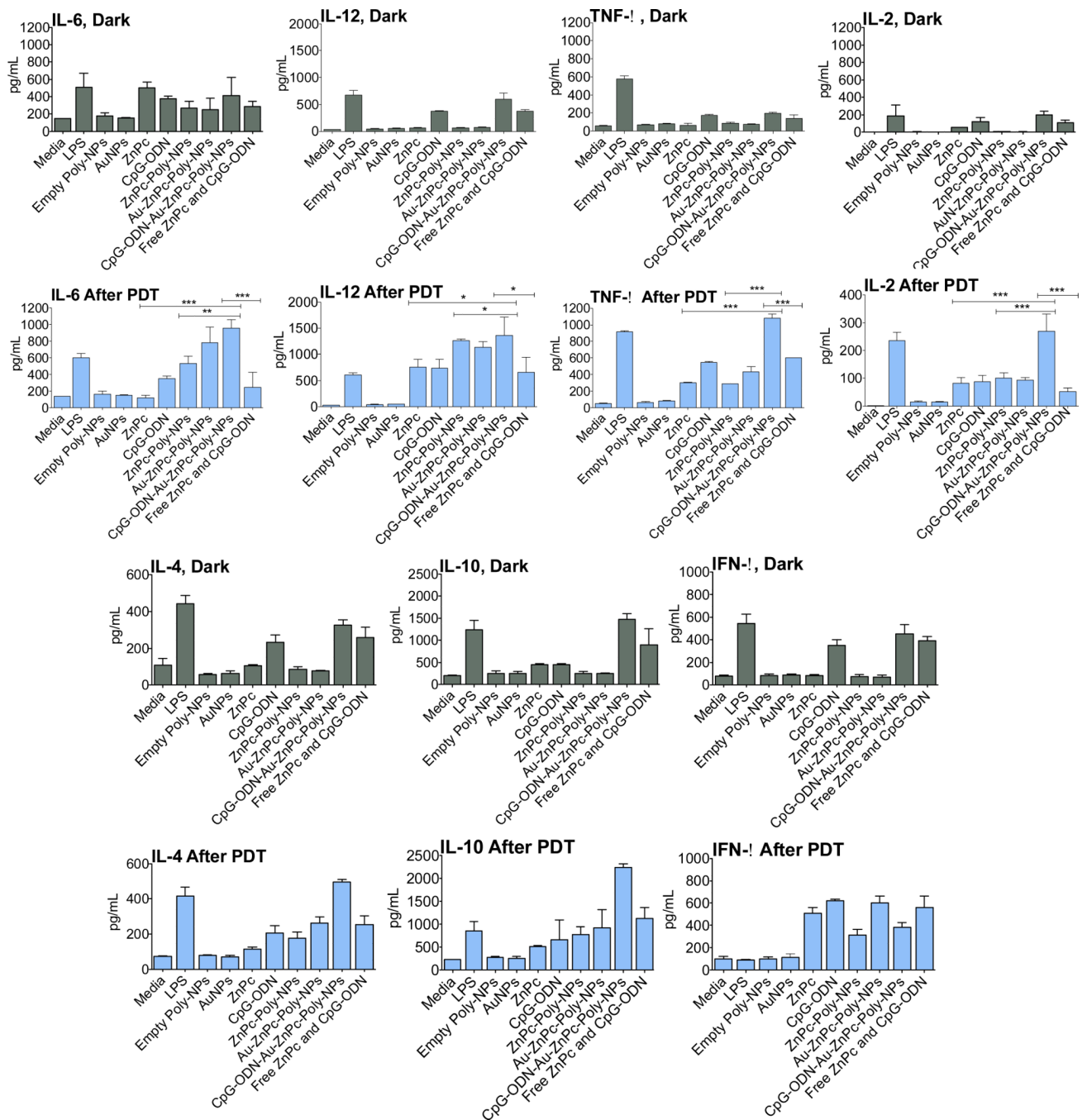


**Fig. 5.** Combination of ZnPc and CpG-ODN in a single NP construct potentiate immune response after PDT. Asterisk represents significant differences between CpG-ODN-Au-ZnPc-Poly-NPs, ZnPc-Poly-NPs, free ZnPc, and a 1:1 combination of free ZnPc and CpG-ODN according to one-way ANOVA with Tukey post hoc test. Single, double, and triple asterisks indicate a P value < 0.05, < 0.004, and < 0.001, respectively.